

# ELECTROGENERATIVE PROCESS FOR THE RECOVERY OF GOLD FROM CYANIDE SOLUTIONS AND THE FORMATION OF GOLD MICROSTRUCTURES ON CARBON- BASED MATRICES

By

YAP CHIN YEAN

June 2010

ELECTROGENERATIVE PROCESS FOR THE  
RECOVERY OF GOLD FROM CYANIDE  
SOLUTIONS AND THE FORMATION OF GOLD  
MICROSTRUCTURES ON CARBON-BASED  
MATRICES

By

YAP CHIN YEAN

Thesis submitted in fulfillment of the requirements for  
the degree of  
Doctor of Philosophy

June 2010

## **ACKNOWLEDGEMENTS**

I would like to express my gratitude and appreciation to the following individuals and groups for their support and contribution to this work:

Prof. Norita Mohamed for her supervision, guidance and constant encouragement which made this studies successful.

Dr. Hamzah Darus for his inspiration and valuable suggestions to this research.

All members of Prof. Norita's research group, Mashita Abdullah, Norazlina Aminuddin, Poh Wan Hui and fellow lab members and graduate students who were not listed here for their friendship, encouragement and valuable help.

Mr Ariffin and all the lab assistants in the School of chemical Sciences, USM for their assistance in laboratory and prompt attention to my requests. Ms Jamillah and Mr Johari from the School of Biological Sciences, USM for their help during SEM measurements.

Ministry of Science, Technology and Innovation (MOSTI) Malaysia for a postgraduate research scholarship.

Mr Teoh Tiong Sean, my husband who is always standing by me, understanding and believing in me.

My friends, my parents and my brother for their love and unwavering support, gave me strength to complete this degree program.

## TABLE OF CONTENTS

ACKNOWLEDGEMENT	ii
TABLE OF CONTENTS	iii
LIST OF TABLES	viii
LIST OF FIGURES	ix
LIST OF SYMBOLS	xv
ABSTRAK	xvii
ABSTRACT	xix

CHAPTER 1 INTRODUCTION	1
1.1 Metal Ions Removal and Recovery from Process Solutions	1
1.2 Electrogenative System and its Working Principle	6
1.3 Electrogenative Reactors	7
1.3.1 Reactor Design and Operation Modes	9
1.3.1.1 Flow-through and flow-by Reactor	9
1.3.2 Three-dimensional Electrodes	13
1.3.2.1 Porous Graphite	13
1.3.2.2 Reticulated Vitreous Carbon	15
1.3.3 Electrochemical Reactor Design with Three-dimensional Electrodes	17
1.3.4 Ion Exchange Membrane	21
1.3.5 Electrochemical Transport Process	21
1.3.5.1 Charge Transfer and Kinetics	22
1.3.5.2 Mass Transport	24
1.3.5.3 Interaction between Charge Transfer and Mass Transport	25
1.3.6 Simple Batch Reactor	27
1.3.7 Batch-recycle Reactor	28
1.4 Application of Electrogenative Process for Environmental Applications	30
1.4.1 Electrosynthesis of Organic Chemicals by Electrogenative Processes	30

1.4.2	Electrogenerative Leaching of Sulfide Minerals	32
1.4.3	Recovery and Removal of Copper via an Electrogenerative System	32
1.4.4	Removal of Hexavalent Chromium from Industrial Process Solutions	34
1.4.5	Removal of Lead via Galvanic Deposition	35
1.4.6	Electrogenerative Gold Recovery from Cyanide Solutions	36
1.4.6.1	The Chemistry of Gold Recovery from Cyanide Solutions in an Electrogenerative Reactor	37
1.4.6.2	Metals Affecting Gold Recovery from Cyanide Solutions	40
1.5	Electrode Pretreatment with Palladium/tin Activation Solution	43
1.6	Electrodeposition and New Phase Formation	47
1.6.1	Metal Ions Adsorption	48
1.6.1.1	Langmuir Adsorption Model	49
1.6.1.2	Elovich Adsorption Model	49
1.6.2	Three-dimensional Nucleation	50
1.6.2.1	Three-dimensional Nucleation Limited by Diffusional Growth	50
1.6.2.2	Three-dimensional Nucleation Limited by Lattice Incorporation	53
1.6.3	Two-dimensional Nucleation Mechanism	54
1.6.3.1	Two-dimensional Nucleation Mechanism Controlled by Diffusion	54
1.6.3.2	Two-dimensional Nucleation Mechanism Controlled by Lattice Incorporation of the Adatom.	54
1.64	Formation of Gold Nanoparticles and its Catalytic Properties	57
1.7	Objectives	58
CHAPTER 2 EXPERIMENTAL		60
2.1	Equipment	60
2.1.1	Electrogenerative Reactor	60
2.1.1.1	Batch Reactor	60
2.1.1.2	Batch-recycle Reactor	60

2.1.2	Electrode Materials	62
2.1.2.1	Cathode Materials for Electrogenenerative Reactor	62
2.1.2.2	Anode for Electrogenenerative Reactor	64
2.1.2.3	Reference Electrode for Electrogenenerative Reactor	64
2.1.2.4	Electrode for Cyclic Voltammetry and Chronoamperometry Studies	64
2.1.3	Cation Exchange Membrane	69
2.1.4	Potentiostat	69
2.1.5	Multimeters	69
2.1.6	Pumps	69
2.1.7	Resistance Box	70
2.1.8	pH Meter	70
2.1.9	Conductivity Meter	70
2.2	Experimental Procedure	70
2.2.1	Preparation of electrode	70
2.2.1.1	Gold Recovery Studies	70
2.2.1.2	Cyclic Voltammetric and Chronoamperometric Studies	71
2.2.2	Preparation of electrolyte	71
2.2.2.1	Catholyte	71
2.2.2.2	Anolyte	71
2.2.2.3	Modified Shipley Solution	72
2.2.2.4	Gold cyanide solution added with surfactant	72
2.2.3	Experimental Approach	72
2.2.3.1	Electrogenenerative Gold Recovery Studies in a Batch Reactor	75
2.2.3.2	Cathodic Polarization Curves with Batch Reactor	75
2.2.3.3	Electrogenenerative Gold Recovery with A Flow-through Batch-recycle Reactor	76
2.2.3.4	Determination of Kinematic Viscosity of Gold Cyanide Solution	78
2.2.3.5	Voltammetric and Chronoamperometry Studies	78
2.2.3.6	Electrogenenerative Gold Deposition	79

2.2.3.7 Characterization of Deposited Gold	79
CHAPTER 3 RESULTS AND DISCUSSION: BATCH REACTOR	81
3.1 Polarization Studies on the Recovery of Gold from Cyanide Solution	81
3.2 Voltammetric Studies	85
3.3 Electrogenative Gold Recovery	94
3.3.1 Effect of stirring of anolyte	96
3.3.2 Effect of cathode materials	96
3.4. Electrode Pretreatment with Palladium/Tin Activation Solution.	103
3.5 Surface Morphology of Gold Deposits	103
3.5.1 Effect of Different Substrates	103
3.5.2 Effect of Surfactants	109
3.6. Conclusions	112
CHAPTER 4 RESULTS AND DISCUSSION: BATCH-RECYCLE REACTOR	115
4.1 Kinematic Viscosity of Different Concentrations of Gold Cyanide Solution	116
4.2 Voltammetric Studies	116
4.3 Performance of A Batch-recycle Flow-through Reactor	124
4.4 Mass Transport Studies	128
4.5. Conclusions	132
CHAPTER 5 RESULTS AND DISCUSSION: ELECTROCHEMICAL NUCLEATION OF GOLD ONTO RETICULATED VITREOUS CARBON FROM CYANIDE SOLUTIONS	135
5.1 Cyclic Voltammetry of Electrochemically Pretreated RVC for Nucleation Studies	136
5.2 Chronoamperometric Studies - Electrodeposition of Gold onto Non-activated RVC	139
5.3 Electrogenative Deposition of Gold onto Non-activated RVC	148
5.4 Conclusions	151

CHAPTER 6 RESULTS AND DISCUSSION: ELECTROCHEMICAL NUCLEATION OF GOLD ONTO ACTIVATED RETICULATED VITREOUS CARBON FROM CYANIDE SOLUTIONS	153
6.1 Cyclic Voltammetric of Electrochemically Pretreated Activated RVC for Nucleation Studies	153
6.2 Chronoamperometric Studies - Electrodeposition of Gold onto Activated RVC	155
6.2.1 Nucleation Mechanism for deposition potentials from -1.05 V to -1.25 V	162
6.2.2 Nucleation Mechanism for deposition potentials from -1.30 V to -1.50 V	164
6.3 Electrogenative Deposition of Gold onto Activated RVC	174
6.4 Conclusions	177
CHAPTER 7 CONCLUSIONS	181
7.1 Recommendations For Future Research	182
REFERENCES	184
APPENDICES	
Appendix A Details of design and measurement of flow through electrogenerative reactor.	
Appendix B Properties of Ion Exchange Membrane	
Appendix C Experimental Results	
Appendix D List of publications	



## LIST OF TABLES

Table	Page
1.1 Scope of electrochemical techniques.	5
1.2 Standard electrode potentials of metal cyanide complexes in aqueous solutions.	41
1.3 Cumulative formulation constants for metal cyanide complexes.	42
2.1 Properties of grade SG-132 porous graphite.	65
2.2 Physical properties of RVC 80 ppi.	66
2.3 Summary of experimental conditions.	67
2.4 Physico-chemical properties of surfactants and surfactant concentrations in cyanide solution.	73
3.1 Polarization characteristics for different cathode materials in 2.54 mM $\text{KAu}(\text{CN})_2$ in 0.0408 M of NaCN solution.	84
3.2 Cell performance for the gold recovery from 2.54 mM of $\text{KAu}(\text{CN})_2$ in 0.0408 M of NaCN solution with different cathode materials.	102
4.1 Experimental time recorded and the calculated kinematic viscosities of different concentrations of gold cyanide solution.	117
4.2 Kinematic viscosities and diffusion coefficients obtained for different concentration of $\text{KAu}(\text{CN})_2$ in 0.0408 M of NaCN solution at 27 °C.	123
4.3 Values of $k_m A_e$ and $k_m$ taken from the slopes of the $\ln(c_t/c_0)$ against time plots shown in the inset of Figure 4.4 to 4.6.	130
5.1 Best fit parameters obtained from non-linear fitting of Eqs. 5.2 and 5.3 to the experimental current densities recorded during the gold electrodeposition onto RVC at different potentials.	149
6.1 Kinetic parameters obtained by the non-linear fitting of Eq. 6.1 to the potentiostatic transients shown in Figure 6.2	159
6.2 Kinetic parameters obtained by the non-linear fitting of Eq 6.2 to the potentiostatic transients in Figure 6.2	165
6.3 Electron work function of elements.	173
6.4 Kinetic parameters obtained by the non-linear fitting of Eq. 6.1 to the electrogenerative transients in Figure 6.11	178

## LIST OF FIGURES

Figure		Page
1.1	Schematic diagram of an electrogenerative reactor and its electrical circuit.	8
1.2	Flow-by and flow-through reactor configurations.	10
1.3	Parallel flow-by reactor with six electrode pairs (electrical circuits excluded).	11
1.4	Flow-by reactor connected in a series (electrical circuits excluded).	12
1.5	Three dimensional schematic of the graphite structure (Pierson, 1993)	14
1.6	SEM micrograph that shows the three-dimensional honeycomb structure of RVC at 50 x magnification.	16
1.7	Electrode potential and normalized current density distribution in three-dimensional electrodes. (a) thin electrode (b) thick electrode. $j(x)$ is the local current density at point x and $j_{ave}$ is the mean current density over all x (adapted from Pletcher and Walsh, 1992)	19
1.8	Potential distribution in a three-dimensional electrode in (a) flow-through (b) flow-by reactor. Dotted line show solid phase potential in case of an excellent current conductor, ( $\Phi_m = \text{constant}$ )	20
1.9	The $i$ vs E and corresponding $\log i/t^0$ vs $\eta$ characteristics for a redox process, $O + ne^- = R$ (Pletcher, 1992)	26
1.10	Electrochemical processes in an electrogenerative reactor.	38
1.11	Colour changes during preparation of Pd/Sn catalyst solution.	46
2.1	Experimental setup and electrical circuit for a batch reactor.	61
2.2	Schematic diagram of the flow-through electrogenerative reactor.	63
2.3	Outline of experimental approach.	74
2.4	Schematic view of the hydraulic circuit.	77
2.5	Electrical circuit of batch cell connected with E-corder and potentiostat for gold electrogenerative deposition.	80
3.1	Cathodic polarization curves for electrogenerative deposition of 2.54 mM of $\text{KAu(CN)}_2$ in 0.0408 M of NaCN on various substrates, ( $\Delta$ ) activated porous graphite electrode; ( $\nabla$ ) porous graphite electrode; ( $\square$ ) activated RVC 80 ppi electrode; ( $\blacksquare$ ) non-activated RVC 80 ppi electrode; ( $\bullet$ ) stainless steel plate electrode; ( $\circ$ ) copper plate	82

	electrode.	
3.2	Cyclic voltammograms obtained from 2.54 mM of $\text{KAu(CN)}_2$ in 0.0408 M of NaCN solution at $5 \text{ mV s}^{-1}$ on: (—) activated RVC; (— —) non-activated RVC; (·····) 0.0408 M of NaCN solution free of gold ions.	87
3.3	Cyclic voltammogram obtained from (—) 2.54 mM of $\text{KAu(CN)}_2$ in 0.0408 M NaCN solution and (·····) 0.0408 M NaCN background solution on graphite at $10 \text{ mV s}^{-1}$ .	89
3.4	Cyclic voltammogram obtained from (—) 2.54 mM of $\text{KAu(CN)}_2$ in 0.0408 M NaCN solution and (·····) 0.0408 M NaCN background solution on activated graphite at $10 \text{ mV s}^{-1}$ .	91
3.5	Cyclic voltammograms for 2.54 mM of $\text{KAu(CN)}_2$ in 0.0408 M of NaCN solution on copper plate, at (—) $25 \text{ mV s}^{-1}$ ; (— —) $75 \text{ mV s}^{-1}$ ; (— — —) $150 \text{ mV s}^{-1}$ . Cyclic voltammogram for 0.0408 M NaCN solution background solution (·····) on copper plate at $25 \text{ mV s}^{-1}$ were also shown.	92
3.6	Cyclic voltammogram for 2.54 mM of $\text{KAu(CN)}_2$ in aqueous solution on copper plate, $25 \text{ mV s}^{-1}$ .	93
3.7	Cyclic voltammogram for 2.54 mM of $\text{KAu(CN)}_2$ in 0.0408 M of NaCN solution on stainless steel, $10 \text{ mV s}^{-1}$ .	95
3.8	Percent of gold recovery with stainless steel cathode from 2.54 mM of $\text{KAu(CN)}_2$ in 0.0408 M of NaCN solution in 3 h of experiment. (●) with both anolyte and catholyte stirred; (○) with only catholyte stirred. Error bars displayed are standard error of percentage of gold recovery for three replicates.	97
3.9	Percent of recovery vs. time with different cathode substrates from 2.54 mM of $\text{KAu(CN)}_2$ in 0.0408 M NaCN solution in 3 h of experiment. (□) activated RVC 80 ppi electrode; (■) RVC 80 ppi electrode; (○) activated porous graphite electrode; (●) porous graphite electrode; (Δ) stainless steel plate electrode; (▼) copper plate electrode.	98
3.10	Linearization of normalized concentration of gold(I) as a function of time with different cathode materials. (□) activated RVC 80 ppi	100

	electrode; (■) RVC 80 ppi electrode; (○) activated porous graphite electrode; (●) porous graphite electrode; (Δ) stainless steel plate electrode; (▼) copper plate electrode.	
3.11	SEM micrographs of porous graphite activated using Pd/Sn at (a) magnification of 50 x (b) magnification of 1.01 kx	104
3.12	EDX analysis for activated porous graphite shown in Figure 3.11 (b)	105
3.13	SEM micrographs of RVC activated using Pd/Sn at (a) magnification of 50 x (b) magnification of 1kx.	106
3.14	EDX analysis for activated RVC shown in Figure 3.13 (b)	107
3.15	Light microscope photos for gold deposited (a) on activated graphite (b) activated RVC after 1 h of experiment from 2.54 mM of $\text{KAu(CN)}_2$ in 0.0408 M of NaCN solution	108
3.16	SEM micrographs of gold deposited on: (a) copper plate; (b) stainless steel plate; (c) activated porous graphite; and (d) activated RVC 80 ppi with magnification of 10 kx.	110
3.17	Influence of surfactants on the structure of the gold deposits in 1 hour of experiment from 2.54 mM of $\text{KAu(CN)}_2$ in 0.0408 M of NaCN solution (a) without surfactant; (b) Addition of CTAB; (c) Addition of SDS; (d) Addition of Triton X-100 with magnification of 2.5 kx.	111
3.18	Comparison between gold deposits from 2.54 mM of $\text{KAu(CN)}_2$ in 0.0408 M of NaCN solution after 1 hour of experiment. (a) Without surfactant; (b) Addition of CTAB with magnification of 10 kx	113
4.1	Cyclic voltammograms obtained on activated RVC at $5 \text{ mV s}^{-1}$ in: (—) 0.0408 M of NaCN solution with 2.54 mM of $\text{KAu(CN)}_2$ ; (— —) 0.0408 M of NaCN solution with 0.508 mM of $\text{KAu(CN)}_2$ ; (·····) 0.0408 M of NaCN solution with 0.051 mM of $\text{KAu(CN)}_2$ .	118
4.2	Linear sweep voltammograms for gold deposition onto gold electrode in a solution containing 2.54 mM of $\text{KAu(CN)}_2$ in 0.0408 M of NaCN solution at different scan rates.	120
4.3	Cyclic voltammograms for gold deposition onto activated RVC electrode in a solution containing 2.54 mM of $\text{KAu(CN)}_2$ in 0.0408 M of NaCN solution at different scan rates.	121

4.4	Normalized concentration ( $c_t/c_0$ ) vs. time plots for the recovery from 0.051 mM $\text{KAu(CN)}_2$ in 0.0408 M of NaCN solution on activated RVC cathodes. Inset: Plots of $\ln(c_t/c_0)$ vs. time for the data shown. (●) $1.67 \times 10^{-7} \text{ m}^3 \text{ s}^{-1}$ ; (○) $3.33 \times 10^{-7} \text{ m}^3 \text{ s}^{-1}$ ; (▼) $8.33 \times 10^{-7} \text{ m}^3 \text{ s}^{-1}$ ; (Δ) $1.25 \times 10^{-6} \text{ m}^3 \text{ s}^{-1}$ ; (■) $1.67 \times 10^{-6} \text{ m}^3 \text{ s}^{-1}$ .	125
4.5	Normalized concentration ( $c_t/c_0$ ) vs. time plots for the recovery from 0.508 mM $\text{KAu(CN)}_2$ in 0.0408 M of NaCN solution on activated RVC cathodes. Inset: Plots of $\ln(c_t/c_0)$ vs. time for the data shown. (●) $1.67 \times 10^{-7} \text{ m}^3 \text{ s}^{-1}$ ; (○) $3.33 \times 10^{-7} \text{ m}^3 \text{ s}^{-1}$ ; (▼) $8.33 \times 10^{-7} \text{ m}^3 \text{ s}^{-1}$ ; (Δ) $1.25 \times 10^{-6} \text{ m}^3 \text{ s}^{-1}$ ; (■) $1.67 \times 10^{-6} \text{ m}^3 \text{ s}^{-1}$ .	127
4.6	Normalized concentration ( $c_t/c_0$ ) vs. time plots for the recovery from 2.54 mM $\text{KAu(CN)}_2$ in 0.0408 M of NaCN solution on activated RVC cathodes. Inset: Plots of $\ln(c_t/c_0)$ vs. time for the data shown. (●) $1.67 \times 10^{-7} \text{ m}^3 \text{ s}^{-1}$ ; (○) $3.33 \times 10^{-7} \text{ m}^3 \text{ s}^{-1}$ ; (▼) $8.33 \times 10^{-7} \text{ m}^3 \text{ s}^{-1}$ ; (Δ) $1.25 \times 10^{-6} \text{ m}^3 \text{ s}^{-1}$ ; (■) $1.67 \times 10^{-6} \text{ m}^3 \text{ s}^{-1}$ .	129
4.7	Double logarithmic plots of the specific mass transport coefficient, $k_m A_e$ vs. linear flow velocity, $v$ for gold recovery on activated RVC from different initial gold concentrations in 0.0408 M of NaCN solution. (●) 0.051 mM of $\text{KAu(CN)}_2$ ; (○) 0.508 mM of $\text{KAu(CN)}_2$ ; (▼) 2.54 mM of $\text{KAu(CN)}_2$ .	131
4.8	Double logarithmic plot of dimensionless $Sh/Sc^{0.33}$ vs. $Re$ for gold recovery on activated RVC from different initial gold concentrations in 0.0408 M of NaCN solution. (●) 0.051 mM of $\text{KAu(CN)}_2$ ; (○) 0.508 mM of $\text{KAu(CN)}_2$ ; (▼) 2.54 mM of $\text{KAu(CN)}_2$ .	133
5.1	Cyclic voltammogram obtained in (— —) 0.0408 M of NaCN and (—) 2.54 mM of $\text{KAu(CN)}_2$ in 0.0408 M of NaCN solution system on electrochemically pretreated non activated RVC at $10 \text{ mV s}^{-1}$ . Direction of scan and cross-over potential ( $E_{co}$ ) are also indicated in the figure.	138
5.2	Current-time curves for the deposition of Au onto RVC from 2.54 mM of $\text{KAu(CN)}_2$ in 0.0408 M of NaCN solution at deposition potential -1.1 V to -1.5 V vs. Ag/AgCl.	140

5.3	Current transients for deposition of Au onto RVC at deposition potential -1.1 V to -1.5 V vs. Ag/AgCl plotted in dimensionless form. Also shown are theoretical curves for progressive and instantaneous nucleation.	142
5.4	SEM images for Au deposited on RVC at various step potentials. (a) -1.1 V (b) -1.2 V (c) -1.3 V (d) -1.4 V (e) -1.5 V with magnification of 10 kx.	144
5.5	The plots of the $j$ - $t$ curves analysis for the adsorption process. (a) Elovich adsorption by $j^{-1}$ vs. $t$ (b) Langmuir adsorption by $\ln j$ vs. $t$ .	146
5.6	Comparison of experimental current transients recorded during the deposition of gold at (a)-1.2 V (b) -1.5 V vs. Ag/AgCl with non-linear fitting of the combined nucleation model obtained. The contributions of the different nucleation processes are shown separately.	147
5.7	Experimental current transients and potential transients vs. time during 300 s of electrogenerative gold deposition.	150
5.8	SEM micrograph for Au deposited by electrogenerative deposition for 300 s with magnification of 10 kx.	152
6.1	Cyclic voltammogram obtained from 2.54 mM of $\text{KAu}(\text{CN})_2$ in 0.0408 M NaCN solution on electrochemically pretreated activated RVC at $20 \text{ mV s}^{-1}$ .	154
6.2	Current-time curves for the deposition of Au onto activated RVC from 2.54 mM of $\text{KAu}(\text{CN})_2$ in 0.0408 M NaCN solution at deposition potentials -1.1 V to -1.5 V vs. Ag/AgCl.	156
6.3	Current transients for deposition of Au onto activated RVC at deposition potential -1.05 V to -1.50 V vs. Ag/AgCl plotted in dimensionless form. Also shown are theoretical curves for 2D progressive and instantaneous nucleation.	158
6.4	Current transients for deposition of Au onto activated RVC at deposition potential -1.05 V to -1.50 V vs. Ag/AgCl plotted in dimensionless form. Also shown are theoretical curves for 3D progressive and instantaneous nucleation.	161
6.5	Comparison of experimental current transients recorded during the deposition of gold at -1.1 V vs. Ag/AgCl with non-linear fitting of the	163

	combined nucleation model obtained. The contributions of the different nucleation processes are shown separately.	
6.6	Comparison of experimental current transients recorded during the deposition of gold at -1.5 V <i>vs.</i> Ag/AgCl with non-linear fitting of the combined nucleation model obtained. The contributions of the different nucleation processes are shown separately.	166
6.7	SEM images for Au deposited on activated RVC at -1.3 V after (a) 10 s (b) 20 s (c) 30 s (d) 60 s with magnification of 50 kx.	168
6.8	SEM images for Au deposited on activated RVC at -1.5 V after (a) 5 s (b) 10 s (c) 20 s (d) 30 s (e) 60 s with magnification of 50 kx.	169
6.9	SEM images for Au deposited on activated RVC at various step potentials, $t = 30$ s. (a) -1.1 V (b) -1.2 V (c) -1.3 V (d) -1.4 V (e) -1.5 V with magnification of 10 kx.	170
6.10	EDX spectrum for gold agglomerates on activated RVC.	171
6.11	Experimental current transients and potential transients <i>vs.</i> time during 180 s of electrogenerative gold deposition onto activated RVC.	175
6.12	Comparison of experimental current transients recorded during the electrogenerative deposition of gold with non-linear fitting of the combined nucleation model obtained. The contributions of the different nucleation processes are shown separately.	176
6.13	SEM micrograph for Au deposited onto activated RVC by electrogenerative deposition for 180 s with magnification (a) 10 k x (b) 50 kx.	179

## LIST OF SYMBOLS

$a$	proportional constant
$A$	nuclei rate constant, $s^{-1}$
$A$	effective electrode surface area, $m^2$
$A_s$	active electrode area per unit reactor volume, $m^{-1}$
$A_e$	specific surface area of cathode, $m^{-1}$
$A_x$	cross sectional area, $cm^2$
$b$	Reynolds exponent
$c$	metal concentration, $mol\ cm^{-3}$
$c_O$	concentration of species being oxidize
$c_R$	concentration of species being reduce
$c_0$	initial metal ion concentration, $mol\ cm^{-3}$
$c_t$	metal ion concentration at time t, $mol\ cm^{-3}$
$C$	calibration constant of viscometer, $mm^2\ s^{-2}$
$D$	diffusion coefficient, $cm^2\ s^{-1}$
$E^0$	standard reduction potential, V
$E^0_{cell}$	overall cell potential, V
$E_a$	standard reduction potential at anode, V
$E_c$	standard reduction potential at cathode, V
$E_{co}$	cross-over potential, V
$F$	Faraday's constant, $96485.309\ C\ mol^{-1}$
$\Delta G^0$	standard Gibb's free energy, $kJ\ mol^{-1}$
$h$	height of the monolayer of deposit, cm
$i$	current, A
$i_m$	maximum current, A
$i_p$	peak current, A
$j$	current density, $A\ cm^{-2}$
$j_c$	cathodic current density, $A\ cm^{-2}$
$j_m$	maximum current density, $A\ cm^{-2}$
$j_o$	exchange current density at equilibrium potential, $A\ cm^{-2}$
$k'_g$	vertical growth rate constant, $mol\ cm^{-2}\ s^{-1}$
$k_g$	lateral growth rate constant, $mol\ cm^{-2}\ s^{-1}$
$k_m$	mass transport coefficient, $m\ s^{-1}$



$K$	formulation constant for metal complexes
$M$	atomic weight, $\text{g mol}^{-1}$
$n$	the number electron accepted or release by reaction per mole of reactant
$N$	number of nuclei, $\text{cm}^{-2}$
$N_0$	saturation nucleus density, $\text{cm}^{-2}$
$Q$	volumetric flow, $\text{cm}^3 \text{s}^{-1}$
$Q_{\text{nucl}}$	charge density due to the 2D nucleation process, $\text{C cm}^{-2}$
$R$	correlation coefficient
$R$	universal gas constant, $8.31451 \text{ J K}^{-1} \text{ mol}^{-1}$
$Re$	Reynolds number
$Sc$	Schmidt number
$Sh$	Sherwood number
$t$	time, s
$t_m$	time associated with maximum current, s
$T$	absolute temperature, K
$V_e$	cathode volume, $\text{m}^3$
$V_R$	volume of electrolyte, $\text{m}^3$
$\Phi_m$	local potential in the solid phase, V
$\Phi_s$	local potential in the liquid phase, V
$\alpha$	charge transfer coefficient
$\varepsilon$	porosity of electrode
$\eta$	overpotential, V
$\rho$	density of metal deposit, $\text{g cm}^{-3}$
$\mu$	dynamic viscosity, $\text{kg m}^{-1} \text{s}^{-1}$
$\nu$	kinematic viscosity, $\text{mm}^2 \text{s}^{-1}$
$\nu$	scan rate of the potential, $\text{V s}^{-1}$
$\upsilon$	linear flow velocity, $\text{m s}^{-1}$

# **PROSES ELEKTROGENERATIF UNTUK PEROLEHAN SEMULA EMAS DARIPADA LARUTAN SIANIDA DAN PEMBENTUKAN EMAS MIKROSTRUKTUR PADA MATRIKS BERASASKAN KARBON**

## **ABSTRAK**

Sistem elektrogeneratif telah diperkenalkan sebagai kaedah alternatif untuk perolehan semula emas daripada larutan akueus secara elektrokimia. Proses ini tidak memerlukan bekalan tenaga luar kerana pertukaran kimia berlaku secara spontan, malah pada masa yang sama, tenaga elektrik telah dihasilkan sebagai suatu produk sampingan. Dua jenis mod operasi telah dikaji. Reaktor statik yang beroperasi dalam mod elektrogeneratif telah digunakan untuk perolehan semula emas daripada larutan sianida. Larutan emas sianida digunakan sebagai katolit dalam kajian ini kerana larutan sianida merupakan agen pengekstrakan yang paling biasa digunakan dalam industri hidrometalurgi. Reaktor statik yang dilengkapi dengan katod tiga dimensi iaitu grafit berliang dan karbon kaca berongga (RVC) dan katod dua dimensi iaitu kuprum dan keluli telah digandingkan dengan anod zink. Sistem ini berupaya memperolehi lebih daripada 90% emas dalam masa 3 jam beroperasi. RVC yang diaktifkan merupakan katod yang paling efektif dengan kadar perolehan emas sebanyak 99% dalam satu jam beroperasi. Reaktor elektrogeneratif alir laluan yang dilengkapi dengan RVC yang diaktifkan telah dikaji. Reaktor tersebut mempunyai kadar perolehan emas lebih daripada 99% dalam masa 4 jam beroperasi. Penilaian prestasi reaktor ini adalah berdasarkan kepekatan  $\text{KAu(CN)}_2$  awal dalam larutan sianida iaitu 0.051 mM, 0.508 mM, 2.54 mM dan kadar alir katolit. Berasaskan keadaan eksperimen, kadar perolehan semula emas sangat bergantung kepada kepekatan awal emas dan kadar alir katolit.

Kinetik untuk proses elektropengenaan merupakan gabungan beberapa jenis proses penukleusan yang melibatkan penjerapan, proses penukleusan dua atau tiga dimensi yang dikawal oleh pembauran atau kemasukan kekisi oleh ad-atom. RVC yang diaktifkan dengan larutan Sn/Pd mempunyai saiz partikel yang lebih kecil. Pengaktifan ini menggalakkan proses penukleusan dua dimensi dan nukleus emas akan membentuk di atas tapak aktif Sn/Pd dan tumbuh secara lateral. Pembentukan elektrogeneratif emas menghasilkan saiz emas dalam julat 20-200 nm. Ia boleh digunakan sebagai cara alternatif untuk menghasilkan mangkin emas di atas substrat berongga tiga dimensi.

# **ELECTROGENERATIVE PROCESS FOR THE RECOVERY OF GOLD FROM CYANIDE SOLUTIONS AND THE FORMATION OF GOLD MICROSTRUCTURES ON CARBON-BASED MATRICES**

## **ABSTRACT**

The application of an electrogenerative system as an alternative to the electrochemical recovery of gold from aqueous solutions is presented. This process does not require an external supply of energy due to the spontaneous chemical reaction that takes place in the reactor while generating an external flow of current as a by-product. Two types of operation modes were investigated. A batch reactor operating in an electrogenerative mode is used in gold recovery from cyanide solutions. In this study, gold cyanide solutions serve as the catholyte because cyanide is the most common leachant used during the extraction of metals in the hydrometallurgical industry. The batch reactor with an improved design using three dimensional cathodes namely porous graphite and reticulated vitreous carbon (RVC) and two dimensional cathode materials, copper and stainless steel plates were coupled with a zinc anode. The system resulted in more than 90% gold being recovered within 3 h of operation. Activated RVC serves as a superior cathode material having the highest recovery rate with more than 99% of gold being recovered in 1 h of operation. An electrogenerative flow-through reactor with an activated RVC cathode was also developed. The reactor proved to be efficient in recovering more than 99% of gold within 4 h of operation. The performance of the reactor was evaluated with initial  $\text{KAu(CN)}_2$  concentrations of 0.051 mM, 0.508 mM, 2.54 mM and various electrolyte flow rates. Gold recovery was found to be strongly dependent on electrolyte flow rate and initial gold concentration in the cyanide solution under the experimental conditions used.

The kinetics of the gold electrodeposition process can be described by a combination of different kinds of parallel nucleation processes namely adsorption, two dimensional or three dimensional nucleation process controlled by diffusion or lattice incorporation of ad-atoms. It was found that activation of RVC using Sn/Pd activation significantly decreased the particle sizes and promotes the 2D nucleation process where the gold nuclei will be preferably formed at the Sn/Pd active sites and grow laterally. Electrogenerative gold deposition produced gold deposits with size ranging from 20-200 nm. It could serve as a potential alternative method for gold catalyst formation on 3D microporous substrates.

## **CHAPTER 1 INTRODUCTION**

### **1.1 Metal Ions Removal and Recovery from Process Solutions.**

Metal finishing, electronics and hydrometallurgical industries are major sources of metal ion containing process streams. The report by United States-Asia Environmental Partnership (2002) stated that chemical and electronic industries in Malaysia account for 12% of the country's major industrial polluters. According to the report, the local small to medium electronics and electroplating industries were found to dispose effluents containing heavy metal contaminants into domestic sewage drains without prior treatment. A cost effective treatment system is needed to recover and remove heavy metal ions from the industrial process streams. There is a trend in the metal finishing and processing industries to operate in a close-loop system (Pletcher and Walsh, 1993). The system is designed with complete recycling of excess reagents to ensure maximum utilization and minimal waste generation.

There are several methods available for metal ions removal and recovery from process solutions. Among these techniques, precipitation is the most widely due to its simplicity and cost effectiveness. The solution pH is adjusted to the optimum range for precipitating the metal as a hydroxide. Other reagents such as sulphides are added to increase recovery. Metals such as copper and chromium have been removed from wastewater using precipitation methods. Hexavalent chromium has to be reduced to trivalent chromium by sodium bisulphite or sulphur dioxide (Cherry, 1982). The subsequent process involved adding lime and caustic soda to increase the pH and precipitating the chromium as chromium hydroxide. The process is not selective, hence giving rise to a mixture of different metal precipitates. Treated water

is run through a clarifier to settle the solids. This method generates secondary pollution and involves high cost of sludge disposal in landfills.

Electrodialysis is a process involving an array of ion exchange membranes positioned between a pair of electrodes. The applied voltage drives the flow of ions in solution and the membrane selectively transports ions having positive or negative charges and reject ions of the opposite charge. Removal, separation and pre-concentration of ions can be achieved using this method. The electrodialysis method was applied in removal and recovery of nickel and copper ions from wastewater. (Ogutveran *et al.*, 1997; Spoor *et al.*, 2002; Wong *et al.*, 2002; Cifuentes *et al.*, 2004). Millmam and Heller (1982) demonstrated the successful application of the electrodialysis method in a gold plating operation. Electrodialysis was operated at the drag-out rinse following the plating bath. Ion exchange resins were used for the second rinse to recover the remaining gold. Gold recoveries up to 99% were achieved and the concentrate recovered by electrodialysis was returned directly to the plating tank. However, there is a problem about membrane durability which can potentially increase cost.

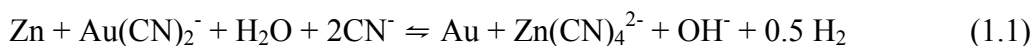
Anion exchange resins have been used for the recovery of gold from cyanide solutions. The solution pH is adjusted and the solution flows through an immobile resin. Ions of interest from the solution are exchanged for similarly charged ions attached to the resin. Although such resins have higher loading capacities than activated carbon, they are much more expensive and their use involves special resin regeneration and elution processes (Gomes *et al.*, 2001). This process has failed to gain wide acceptance compared to adsorption on activated carbon due to its higher

capital cost, poor physical strength of resin and less selectivity. Exhausted resin will need to be incinerated and this process will generate environmentally hazardous fumes.

Adsorption is another method which is widely employed in metal recovery. Gold cyanide or gold chloride complexes are strongly adsorbed on activated carbon (Cho *et al.*, 1979; Adam and Fleming, 1989; Jia *et al.*, 1998). Although the mechanism has not been fully explained, this recovery system has gained wide acceptance in the gold mining industry. Heap leaching of gold with alkaline sodium cyanide in mining industries will typically produce very dilute solutions containing 0.5-10 mg L<sup>-1</sup> of gold(I). The pregnant solution is then transferred to a series of tanks, where carbon is added. The gold is adsorbed onto the surface of the carbon. The carbon, with gold attached, is removed by screening. The gold bearing carbon is then passed through a stripping vessel containing heated sodium hydroxide-cyanide-water solution where the gold is desorbed. After the stripping process, the activated carbon can be regenerated. This preconcentration step will subsequently produce solutions of 50-2500 mg L<sup>-1</sup> of gold(I). Gold ions eluted from the adsorbents are not in their metallic state and will be subjected to electrolytic recovery or cementation (Stavart *et al.*, 1999; Barbosa *et al.*, 2001).

Cementation has been used in metal recovery in hydrometallurgical processes. It is a metal displacement reaction where metal ions from an aqueous solution are precipitated spontaneously by a relatively more electropositive metal. Zinc dust was used in the Merrill-Crowe process to recover gold from cyanide solution. The overall chemical reaction for this process is shown in Eq. 1.1.





The solution is deoxygenated and soluble lead salts are added to the solution to inhibit passivation of the zinc surfaces which increase the cementation rate (Yannopoulos, 1991). Unfortunately, the resulting product is physically inseparable.

In moving towards technologies that are both efficient and environmental friendly, electrochemical methods offer the most promising options. Metal ions can be removed and recovered in a single step. Electrochemical technology plays many important roles in environmental protection and covers a broad range of technologies which are summarized in Table 1.1 (Pletcher, 1992; Pletcher and Walsh, 1993). Electrolytic methods are mostly employed in industries such as in metal refining and recycling or water treatment. However, electrolytic processes have limitations when dealing with low metal ion concentrations. In wastewater treatment and hydrometallurgical processes, the concentration of metal bearing solutions ranges from 1 mg L<sup>-1</sup> to 1000 mg L<sup>-1</sup>. In dilute solutions, the current efficiency of the system is very low due to the side reactions occurring in the system. The power consumption in treating dilute solutions is relatively high and thus it is not cost effective (Pletcher, 1992).

There are numerous research papers dealing with the electrowinning of gold, either from mining industries or electroplating wastes (Stavart *et al.*, 1999; Barbosa *et al.*, 2001; Reyes-Cruz *et al.*, 2002, 2004; Spitzer and Bertazzoli, 2004). Stavart *et al.* (1999) used three-dimensional carbon felt for electrowinning gold where

Table 1.1 Scope of electrochemical techniques.

Scope and details
<p>Metal Extraction, refinery, and production</p> <ul style="list-style-type: none"> <li>Extraction of precious metals from sulphide ores, electrorefining of copper, lead, silver, nickel, electrowinning, cementation, aluminum recycling.</li> </ul>
<p>Water treatment</p> <ul style="list-style-type: none"> <li>Effluent treatment: Removal of toxic metals or organic chemicals from industrial waste streams using electrodialysis or electrolysis techniques prior to discharge.</li> <li>Water disinfection: Ozonation, chlorination, hydrogen peroxide for removal of bacteria.</li> <li>Recycling of process stream: Aim to regenerate redox reagents in the industrial process to achieve 'zero effluent'.</li> </ul>
<p>Metal finishing and materials processing</p> <ul style="list-style-type: none"> <li>Electroplating and electroless deposition, conversion coating forming suitable passive films such as in anodizing and chromating. Electroforming, electrochemical etching and cleaning.</li> </ul>
<p>Selective Chemical synthesis</p> <ul style="list-style-type: none"> <li>Chlor/alkali manufacturing processes, organic electrosyntheses such as hydrodimerization of acrylonitrile, reduction of carboxylic acid.</li> </ul>
<p>On site generations of chemicals</p> <ul style="list-style-type: none"> <li>Chlorine and hydrogen peroxide can be generated on site avoiding hazards of transporting chemicals.</li> </ul>
<p>Cleaner energy generation</p> <ul style="list-style-type: none"> <li>Fuel cells, solar photovoltaic cells.</li> </ul>
<p>Sensors</p> <ul style="list-style-type: none"> <li>Electrochemical sensors are available for a wide range of gases in atmosphere such as CO, SO<sub>2</sub>, NH<sub>3</sub>, NO<sub>x</sub></li> </ul>

Sources: Pletcher, 1992; Pletcher and Walsh, 1993

gold extraction higher than 90% and current efficiencies ranging from 6% to 12% were achieved. Spitzer and Bertazzoli (2004) used a filter-press type electrochemical reactor to recover silver and gold selectively from electroplating effluents. Current efficiencies were found to be 15%-23%. Reyes-Cruz *et al.* (2004) studied gold and silver recovery from a three-dimensional electrochemical reactor with RVC electrodes and recovered 26% gold and 48% silver. All these treatment technologies are categorized as electrolytic cells, which need power consumption. Electrolytic systems involving low concentrations of gold will have kinetics and thermodynamics limitations even though the conductivity of the solution is high. Side reactions such as oxygen and water reduction tend to occur which cause low current efficiencies in all these systems (Reyes-Cruz *et al.*, 2004; Spitzer and Bertazzoli, 2004). An alternative for electrochemical methods that can reduce operating cost for the precious metal recovery process would be the electrogenerative system. This method enables recovery of metals without any external supply of energy.

## 1.2 Electrogenative System and its Working Principle

An electrogenerative reactor is a galvanic reactor. The galvanic process is an electrochemical process in which a chemical reaction that occurs in a system produces an electrical current. The equilibrium potential is obtained by subtracting the potential of cathode to anode and is related to the free energy of the overall cell reaction by following Eq. 1.2

$$\Delta G^{\circ} = -nFE^{\circ}_{\text{cell}} = -nF(E_c - E_a) \quad (1.2)$$

where  $\Delta G^0$  is the Gibbs free energy,  $n$  is the number electrons accepted or released by the reaction per mole of reactant,  $F$  is Faraday's constant,  $E_{\text{cell}}^0$  is the overall cell potential,  $E_c$  is the standard reduction potential at cathode,  $E_a$  is the standard reduction potential at anode.

All electrogenerative processes have a negative Gibbs free energy ( $\Delta G < 0$ ) which means that they are thermodynamically favorable and are spontaneous redox reactions. As with all electrochemical techniques, the electrogenerative reactor is an elegant technology as the main reagent being the electron is a clean reagent.

### **1.3 Electrogenerative Reactors**

Electrogenerative reactors incorporate two coupled electrode reactions. The electrical circuit is shown in Figure 1.1. The electrical contact is made through an external wire and current collectors attached to the anode and cathode. A voltmeter is used to measure the overall cell voltage. Generally, by the careful choice of anode and cathode materials, any redox reaction which is thermodynamically favourable can be utilized for metal recovery. Selectivity and the rate of the reaction can be controlled by varying the electrode potential using a resistance load in the circuit, using suitable electrodes and electrocatalysts. In electrolytic cells, the selectivity of the system depends on the cathode potential applied to the electrode. Electrogenerative processes can be made selective for particular reactions from the choice of electrodes and electrolytes used by the system.

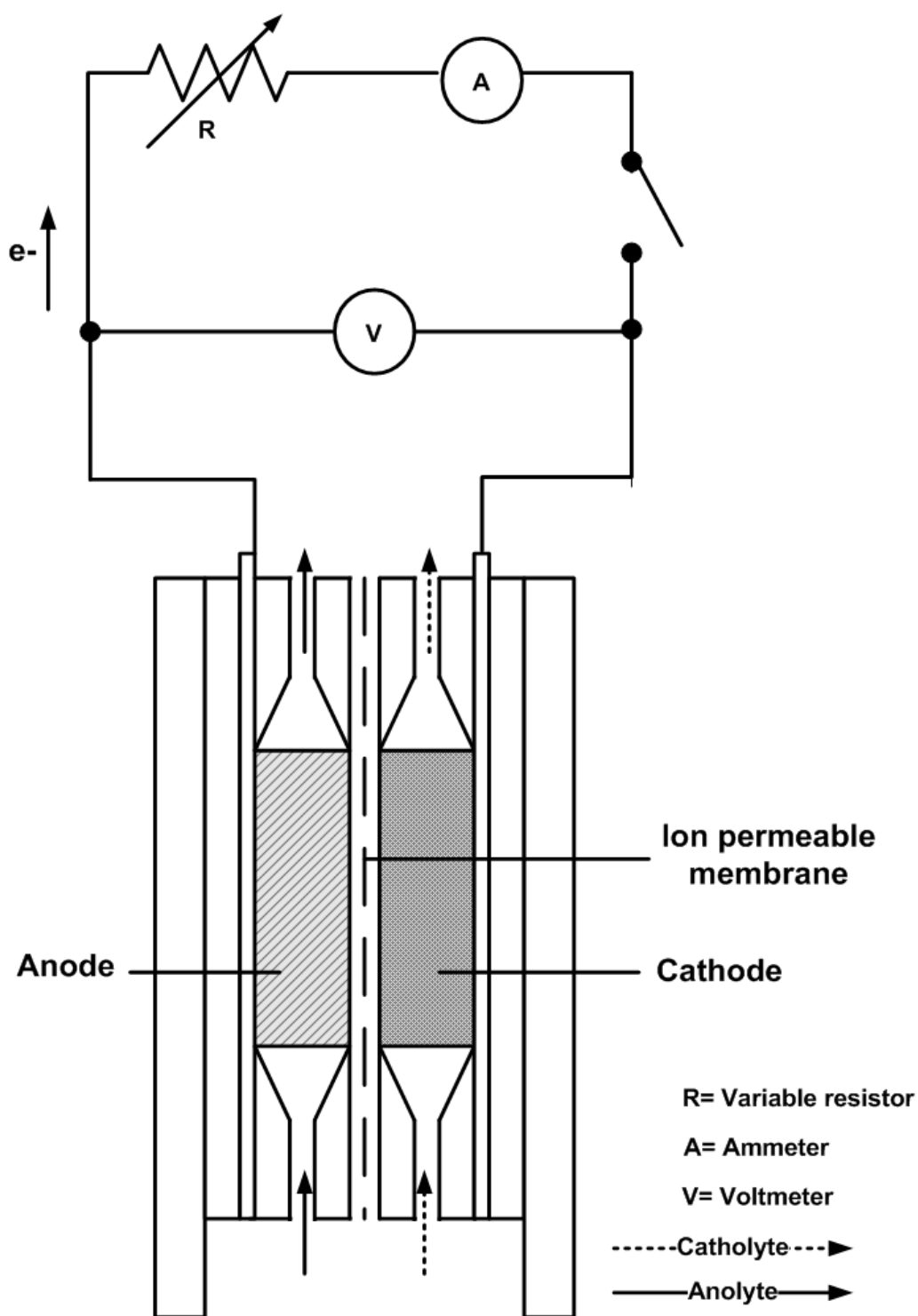


Figure 1.1 Schematic diagram of an electrogenerative reactor and its electrical circuit.

### **1.3.1 Reactor Design and Operation Modes**

Operation of electrogenerative reactors involves many of the concepts of fuel cells and the factors considered in electrolytic cell design can also be applied to electrogenerative reactors. Electrogenerative reactors can be operated in a batch or continuous mode such as a batch reactor, single-pass reactor and batch-recycle reactor.

#### **1.3.1.1 Flow-through and Flow-by Reactor**

The flow reactor can be classified in two groups: flow-through or flow-by systems (Pletcher and Walsh, 1992). The classification is based on the direction of solution flow with respect to the electrical current through the anode and cathode. When the direction of the solution flow and electrical current flow is perpendicular to each other, it is called a flow-by system. If these directions are parallel to each other, it is called a flow-through system. Figure 1.2 shows the schematic diagram of a flow-through and a flow-by system with respect to the directions of current and solution flow. The reactors shown in Figure 1.2 contain two compartments in the cell assembly. The reactor can be assembled with multiple electrode pairs or multiple reactors which can be connected in series or in parallel to increase cell performance. The configurations of the reactor in which the electrode pairs are in parallel and in series are shown in Figure 1.3 and Figure 1.4 respectively.

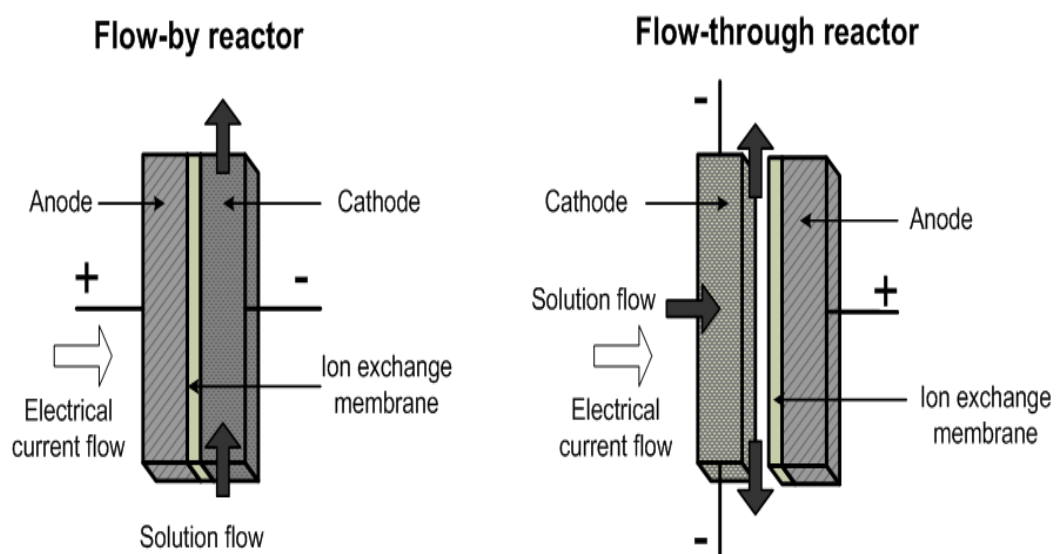


Figure 1.2 Flow-by and flow-through reactor configurations.

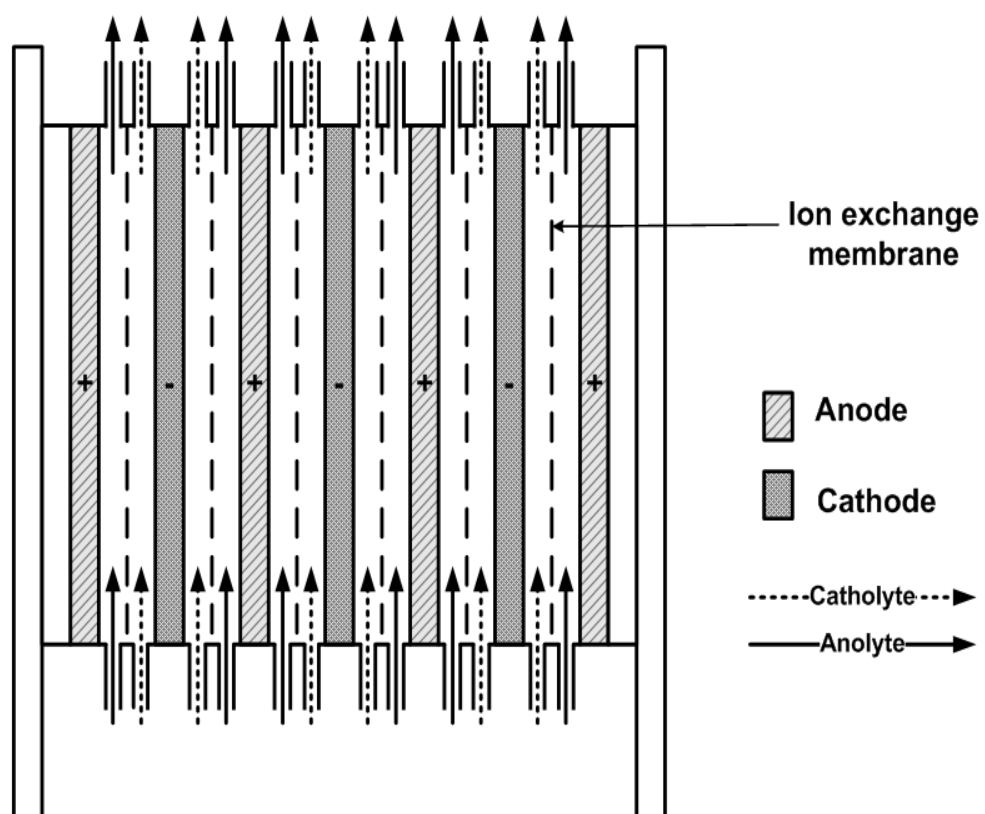


Figure 1.3 Parallel flow-by reactor with six electrode pairs (electrical circuits excluded).



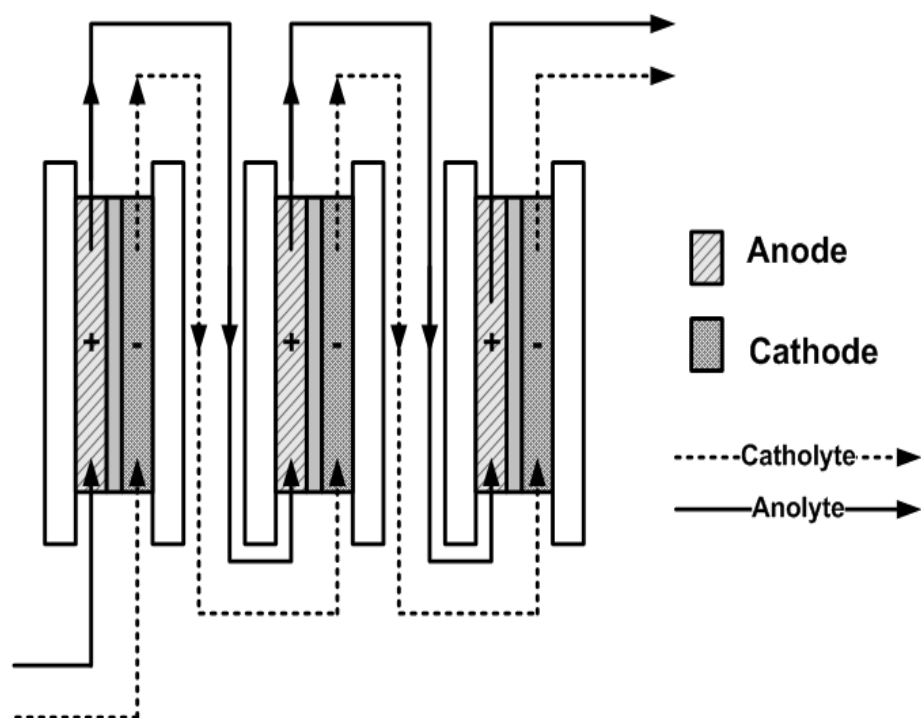


Figure 1.4. Flow-by reactor connected in series (electrical circuits excluded).

### 1.3.2 Three-dimensional Electrodes

The most important component in the electrochemical reactor is the electrode. The electrode can be broadly classified into two types, namely two or three-dimensional electrodes. These electrodes can be static or moving such as the rotating cylinder or rotating disc electrode. High mass transfer rates can be achieved with electrode movement while high surface area can be achieved with the use of porous, three-dimensional electrodes. Three-dimensional electrodes are more superior compared to two-dimensional electrodes when dealing with dilute process liquors due to the higher active electrode area per unit reactor volume leading to higher mass transfer rates even at low metal ion concentrations (Pletcher and Walsh, 1992; Walsh and Reade, 1994; Walsh, 2001). Examples of three-dimensional electrodes are porous graphite electrodes, carbon felts, reticulated vitreous carbon (RVC), packed bed electrodes and active fluidized bed electrodes. Studies involving these three-dimensional electrodes can be found extensively in the literature (Pletcher *et al.* 1991; Ponce-de- Leon and Pletcher, 1996; Widner *et al.* 1998).

#### 1.3.2.1 Porous Graphite

Graphite is one of the allotropes carbon. It is composed of a series of stacked parallel layer planes shown schematically in Figure 1.5. Within each layer plane, each carbon atom is bonded to three others with  $sp^2$  bonding, forming a series of continuous hexagons in what can be considered as an essentially infinite two-dimensional molecule. The hybridized fourth valence electron is paired with another delocalized electron of the adjacent plane by a van der Waals bond. Graphite can conduct electricity due to the vast electron delocalization within the carbon layers. These valence electrons are free to move and hence able to conduct electricity.

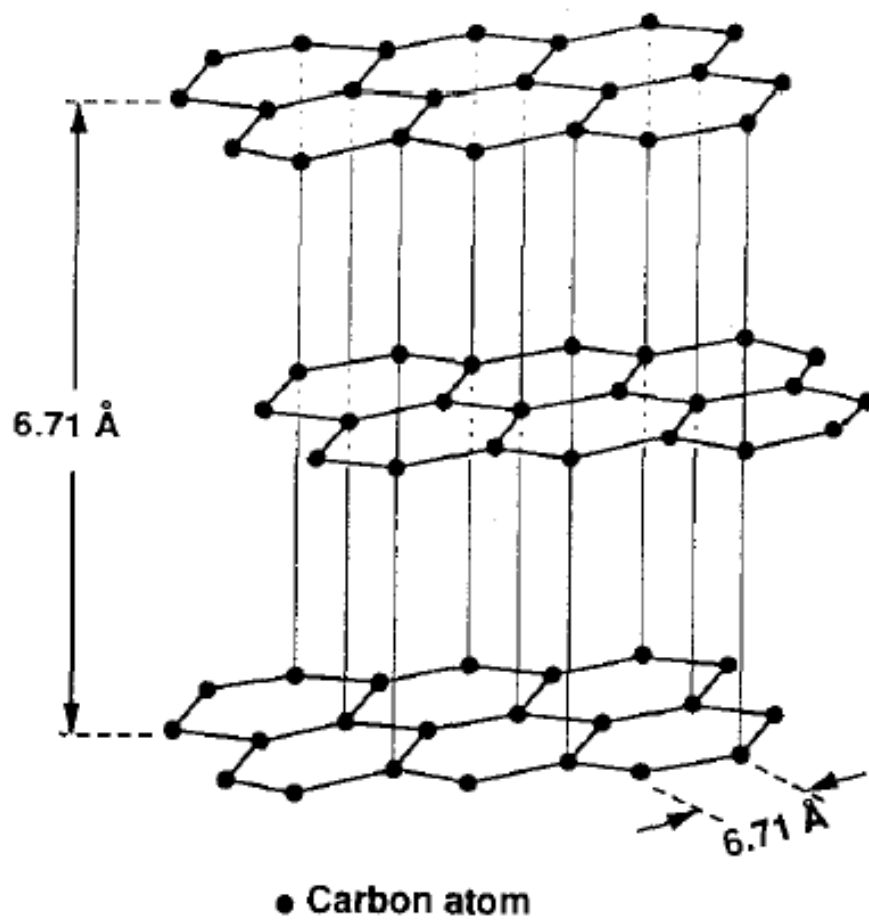


Figure 1.5 Three-dimensional schematic of the graphite structure (Pierson, 1993)

However, the electricity is only conducted within the plane of the layers. There are two known forms of graphite, *alpha* (hexagonal) and *beta* (rhombohedral) graphite which have very similar physical properties except that stacking of these layer planes occurs in two different ways (Pierson, 1993).

### 1.3.2.2 Reticulated Vitreous Carbon

RVC is an open pore foam material composed solely of vitreous carbon (Reticulated vitreous carbon- A new form of carbon, 2008). It has a honeycomb structure as shown by Figure 1.6. The structure of RVC is achieved by polymerisation of resin combined with foaming agents, followed by carbonisation. RVC is produced in several pore sizes, usually described as number of pores per inch (ppi). It has a free void volume between 90% and 97%, depending on the ppi grade and its three-dimensional porous structure offers high surface area, up to  $66 \text{ cm}^2/\text{cm}^3$  for the 100 ppi RVC (Wang, 1981; Friedrich *et al.*, 2004). It is suitable to use RVC as an electrode material especially in flow reactors which require high void volume, high surface area and low electrical and fluid flow resistance. RVC is one of the most chemically inert forms of carbon over a wide range of temperatures. Its chemical inertness, its wide range of usable potential (1.2 to -1.0 V vs. SCE) and the hydrodynamic and structural advantages of its open-pore foam structure make vitreous carbon foam an attractive material for electrodes (Wang, 1981). However, the skeletal structure of the material is brittle and needs support and the low volumetric carbon content means that care has to be taken to ensure uniform potential and current distribution through the material.

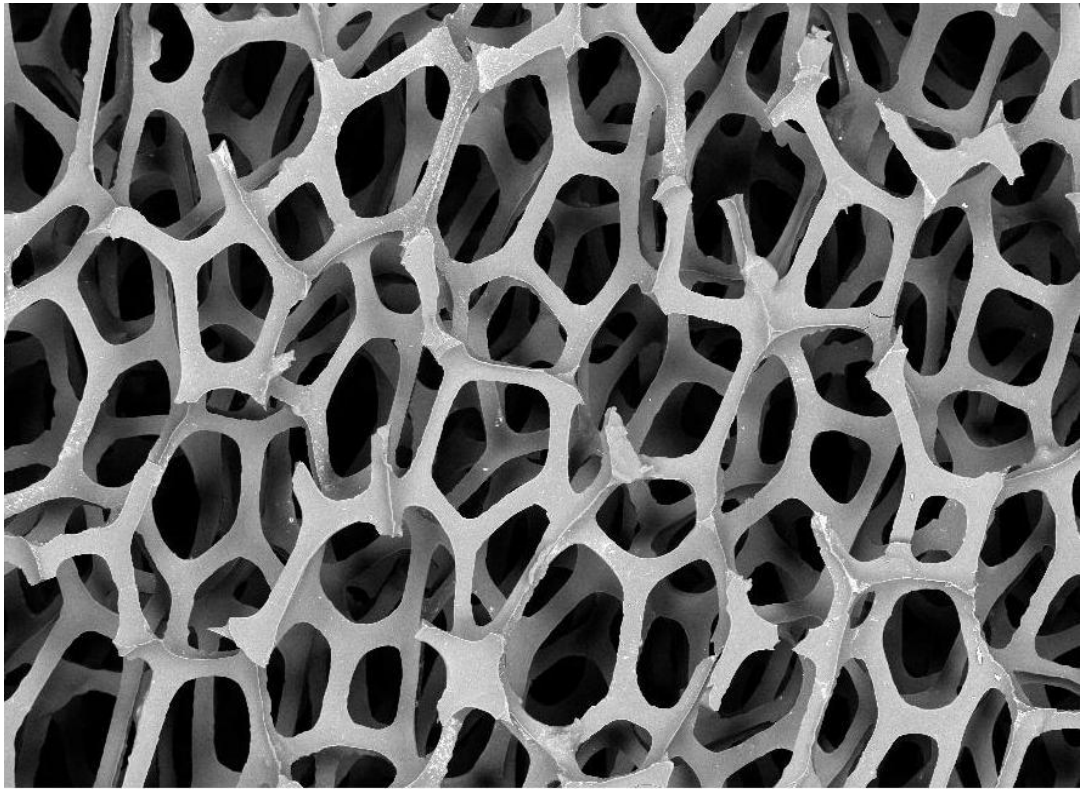


Figure 1.6 SEM micrograph that shows the three-dimensional honeycomb structure of RVC at 50x magnification

### **1.3.3 Electrochemical Reactor Design with Three-dimensional Electrodes**

In electrochemical reactor design, achievement of efficient mass transport is necessary since the maximum current density for a reaction is directly proportional to mass transport coefficient. Efficient mass transport will minimize the differences in the composition of chemical species adjacent to electrode surface and bulk solution. The rate of reaction in a mass transport controlled process depends on the rate at which a particular species reaches the electrode surface. A high mass transport coefficient is favourable when dealing with dilute solutions. Apart from increasing the volumetric flow rate of the electrolyte passing through the reactor, mass transport can be increased by installation of turbulence promoters placed in the flow path of electrolyte. The turbulence promoters can increase local eddy currents and increase mass transport. Turbulence promoters also encourage uniform current and potential distributions by promoting mixing between the boundary layer and the bulk solution (Pletcher, 1992).

The charge transport within an electrolyte solution depends on ionic conduction. The ionic conduction is described by physicochemical laws and quantities, where conductivity, ionic dissociation, ion mobility and transport number are each playing their own roles. The charge transport process also influences the current distribution on the electrode in the reactor. A non-uniform current density will decrease the current efficiency in the process. The main factors which influence current distribution is conductivity of the electrolyte, geometry and dimension of the electrode, activation overpotential at the electrode which depends on electrode kinetics and concentration overpotential which depends on the mass transport process. Because the potential distribution within an electrode is strictly correlated

with current distribution and the selectivity of redox reactions depends strongly on the potential applied to the surface, it is essential to ensure uniformity of the current distribution to increase current efficiency (Heitz and Kreysa, 1986).

The use of three-dimensional electrodes increases the reactor design complexities due to its non-uniform current and potential distribution (Pletcher and Walsh, 1992; Walsh, 2001). The performance of an electrochemical cell using a three-dimensional electrode is critically dependent on the potential distribution within the electrode and penetration depth of the current. The potential in the liquid phase,  $\Phi_s$  and solid phase,  $\Phi_m$  tend to be non-uniform along the direction of current flow, due to the ohmic drop. In thin electrodes, the potential falls slowly, the driving force ( $\Phi_m - \Phi_s$ ) for electrochemical reaction becomes smaller towards the current collector (Figure 1.7 (a)). If the electrode is thick, the driving force will become so small that the reaction rate is under mixed or charge control and the current is very low (Figure 1.7 (b)).

Figure 1.8 shows that the potential distribution arises due to differences in liquid phase potential,  $\Phi_s$  and solid phase potential,  $\Phi_m$  in flow-through and flow-by reactors. For a flow-through porous electrode, if the electrode thickness is higher than effective penetration depth, theoretically very little of the porous electrode is operating under mass transport limiting conditions. Therefore, the effective electrode thickness is limited by a voltage drop. In a flow-by configuration, an ohmic drop occurs across the electrode thickness, electrode length can be extended to achieve a higher conversion per solution pass. It is important to note that distribution of potential, current density and flow are all interrelated in a three-dimensional

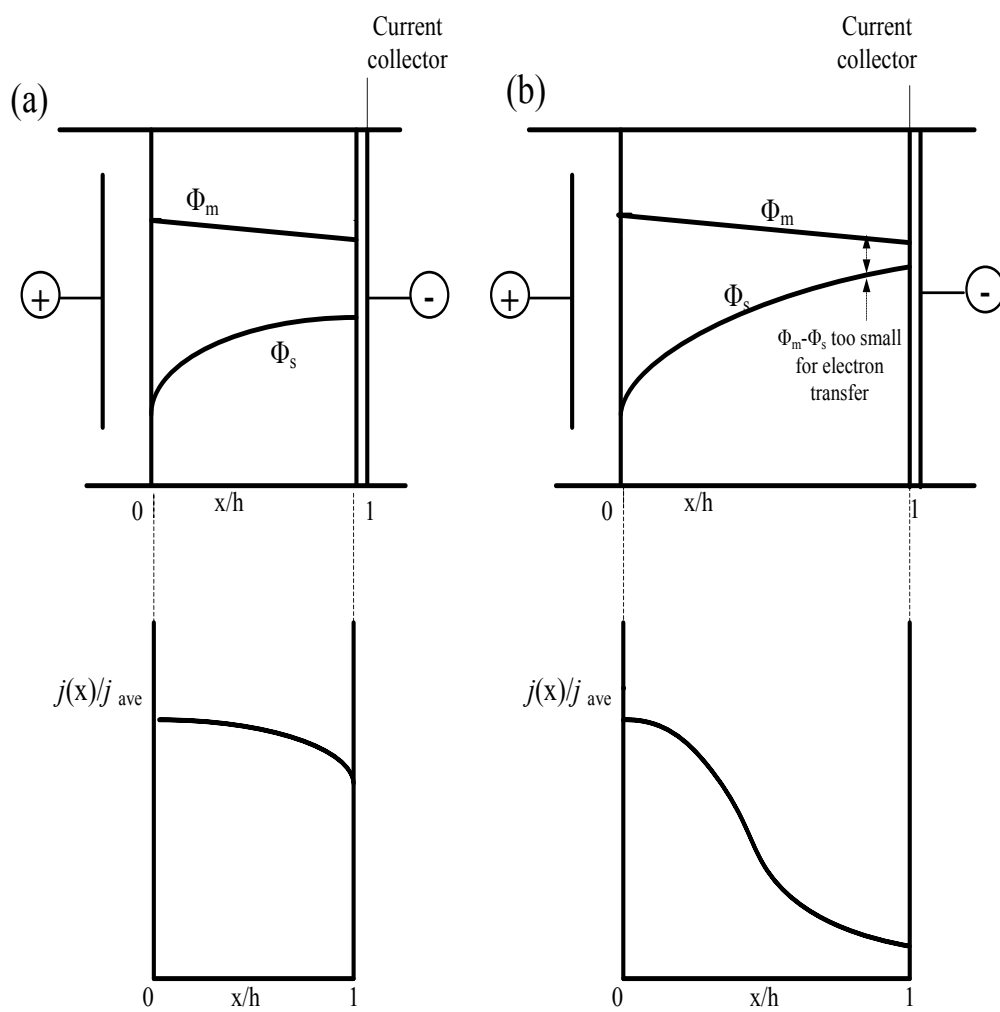


Figure 1.7 Electrode potential and normalized current density distribution in three-dimensional electrodes. (a) thin electrode (b) thick electrode.  $j(x)$  is the local current density at point  $x$  and  $j_{ave}$  is the mean current density over all  $x$  (adapted from Pletcher and Walsh, 1992)



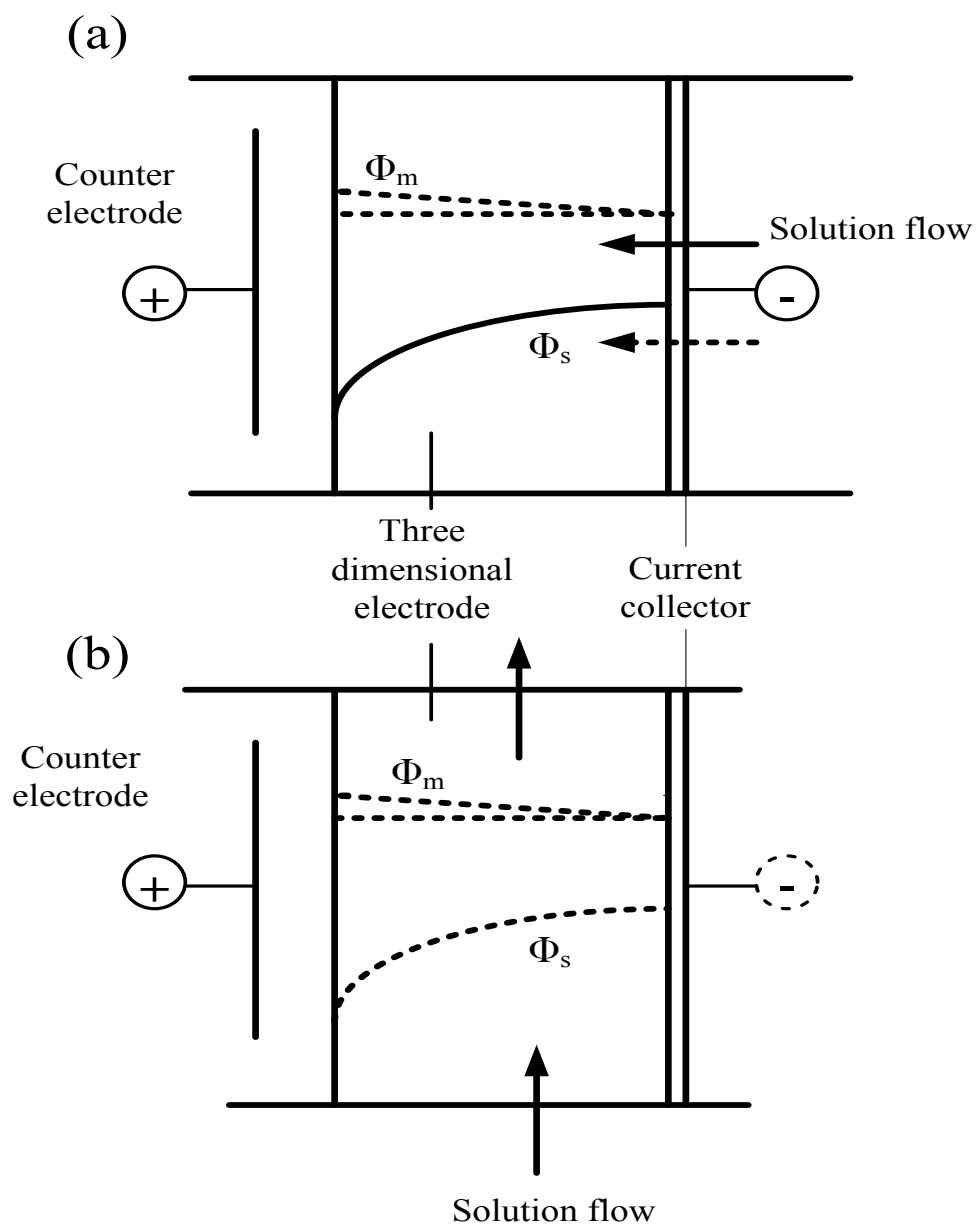


Figure. 1.8 Potential distribution in a three-dimensional electrode in (a) flow-through (b) flow-by reactor. Dotted line shows solid phase potential in case of an excellent current conductor, ( $\Phi_m = \text{constant}$ )

electrode (Langlois and Coeuret, 1990; Pletcher and Walsh, 1992; Doherty *et al.*, 1996).

#### **1.3.4 Ion Exchange Membrane**

Another component which plays an important role in electrogenerative reactors is the ion exchange membrane. It works as a separator between the anolyte and catholyte of different compositions which enforces selectivity in the migration of ions between both compartments. The advantages of using ion permeable membranes as a separator are its high selectivity, high stability and high rate of transport of ions through the membrane thus achieving high conductivity with low resistance (Davis *et al.*, 1997). Other considerations involve the cost of the reactor, low maintenance requirements, simplicity of design and installation, safety and ease of operation. Placement of an ion exchange membrane in the reactor should be considered carefully to minimize the interelectrode gap, which leads to an ohmic loss. The cell design and operation mode are strongly dependent on the specific process application and objective of the operation.

#### **1.3.5 Electrochemical Transport Process**

Heterogeneous reduction of metal ions on the electrode will involve various transport processes. Mass transport, charge transfer processes must be taken into account in the studies of electrochemical reactors. Charge transfer determines the kinetics of the electrochemical reaction. Mass transport describes the transport of chemical species towards and away from the electrode surface; meanwhile charge transfer determines the current distribution in a reactor, influence the space time yield and the scale-up of electrochemical cell (Heitz and Kreysa, 1986).

### 1.3.5.1 Charge Transfer and Kinetics

The kinetics of an electrochemical process depends on the relationship between cell potential and current. The equilibrium potential is obtained by subtracting the potential of cathode to anode and is related to the free energy of the overall cell reaction as indicated by Eq 1.2.

However, Eq 1.2 does not taken into account the rate of reaction. The rate of reaction depends on the kinetics of the two electrode reactions. At equilibrium, the potential of an inert electrode in a solution containing both species O and R will be given by the following Nernst equation;

$$E = E^{\circ} + \frac{RT}{nF} \ln \frac{c_O}{c_R} \quad (1.3)$$

When a potential other than the equilibrium potential is imposed on the electrode, current will pass and the ratio of  $c_O/c_R$  will change according to the Nernst equation. If the electrode is made positive with respect to  $E$ , anodic current will flow and if it is made negative with respect to  $E$ , a cathodic current which is due to the conversion of O to R will be observed. Since oxidation and reduction depend on the charge transfer across the electrode and electrolyte interface, the rate constant for the reaction will be influenced by the local potential field which drives the charge transport. When an electrochemical reaction is slow, an overpotential is needed to drive the reaction. There exists an exponential relationship between current density and overpotential. The measured current is described by Butler-Volmer the equation shown as below;

$$j = j_o \left( \frac{\exp((1-\alpha)nF\eta)}{RT} - \frac{\exp(-\alpha nF\eta)}{RT} \right) \quad (1.4)$$

Where  $j_o$  is exchange current density at the the equilibrium potential,  $\alpha$  is charge transfer coefficient and  $\eta$  is overpotential. This equation shows that the kinetics of charge transfer depend on potential. Some electrode reactions are fast and give a reasonable current density close to the equilibrium potential. In contrast, others are slow and an overpotential is necessary to obtain a required current density. In most practical conditions, the potential will not be close to the equilibrium condition, one of the terms in this equation will be dominant. When the applied potential is negative with respect to equilibrium potential, the equation for the cathodic current becomes as follows;

$$-j_c = j_o \exp\left(\frac{-\alpha nF}{RT} \eta\right) \quad (1.5)$$

The equation can be written as:

$$\log j = \log j_o - \frac{\alpha nF}{2.3RT} \eta \quad (1.6)$$

which is also known as cathodic Tafel equation (Bard and Faulkner, 1980; Pletcher, 1992; Pletcher and Walsh, 1993).

### **1.3.5.2 Mass Transport**

There are three forms of mass transport, namely diffusion, convection and migration (Pletcher, 1992). Diffusion is the movement of species down a concentration gradient and it is described by Fick's Law. An electrochemical reaction converts a reactant to a product at the surface of the electrode. There is a boundary layer adjacent to the electrode surface where the concentration of reactants and products in the boundary layer is lower and higher than the bulk solution respectively. Hence, reactants will diffuse from the bulk solution to the electrode surface and products will diffuse away from it.

Convection is the movement of species due to mechanical forces. It is normally induced by stirring of solutions, electrode rotation and electrolyte flowing through the reactor. Convection can be categorized as free and forced convection. If it is caused by external influence such as stirring, it is called forced convection; whereas if it occurs spontaneously due to temperature variations, it is called free convection.

Migration is the movement of charged species due to a potential gradient. The current of electrons through an external circuit must be balanced by the passage of ions through the membrane. If the reaction is carried out in a high concentration of inert electrolyte in solution, most of the charges will be carried by those inert species and less of the electroactive species is transported by migration.